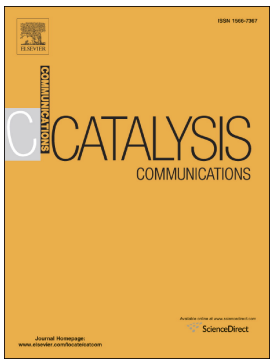

Influence of the preparation method on the performance of Ni-based bifunctional catalysts in the one-pot conversion of γ-valerolactone to valeric biofuel

Karla G. Martínez Figueredo, Darío J. Segobia, Nicolás M. Bertero

PII: S1566-7367(20)30163-1

DOI: https://doi.org/10.1016/j.catcom.2020.106087

Reference: CATCOM 106087

To appear in: *Catalysis Communications*

Received date: 20 April 2020

Revised date: 10 June 2020

Accepted date: 12 June 2020

Please cite this article as: K.G. Martínez Figueredo, D.J. Segobia and N.M. Bertero, Influence of the preparation method on the performance of Ni-based bifunctional catalysts in the one-pot conversion of γ-valerolactone to valeric biofuel, *Catalysis Communications* (2019), https://doi.org/10.1016/j.catcom.2020.106087

Influence of the preparation method on the performance of Ni-based bifunctional catalysts in the one-pot conversion of γ-valerolactone to valeric biofuel

Karla G. Martínez Figueredo, Darío J. Segobia, Nicolás M. Bertero*

Catalysis Science and Engineering Research Group (GICIC), Instituto de Investigaciones en Catálisis y Petroquímica (INCAPE), UNL-CONICET, Centro Científico Tecnológico, Paraje El Pozo, Santa Fe (3000), Santa Fe, Argentina.

*Corresponding author. Fax: +54 342 451 1546; E-mail: nbertero@fiq.unl.edu.ar

Abstract

In this work the one-pot production of pentyl valerate (PV) from γ-valerolactone (GVL) and pentanol in liquid phase at 523 K, 10 bar of H_2 over Ni-based catalysts supported on SiO_2-Al_2O_3 (SA) was studied. By using incipient wetness impregnation (I) and precipitation-deposition (PD) two different catalysts were prepared, characterized and tested in reaction. With larger Ni^0 particles and a significantly higher acid site density, Ni/SA-I was more active and selective to PV, revealing the crucial impact of preparation method on the catalytic performance. After 24 h, a GVL conversion of 83.5% with PV selectivity of 87.8% was reached with Ni/SA-I.

Keywords: preparation method; Ni catalysts; γ-valerolactone; pentyl valerate; biofuel

1. Introduction

The increasing concern about environment and energy issues related to growing greenhouse gas emissions and the depletion of conventional fossil resources has motivated to the scientific society to develop promising alternatives to fossil fuels in the near future. In this sense, lignocellulosic biomass has been identified as a promising feedstock due to the fact that it is abundant, relatively cheap and renewable [1][2]. The increasing number of works reporting the transformations of different biomass-derived raw materials into γ-valerolactone (GVL) confirm that this lactone is becoming a strategic renewable platform molecule [3] and the exploration of new technological processes for obtaining biofuels starting from GVL are of considerable interest for the transportation sector [4][5][6].

Regarding biofuel properties, valerate or valeric esters have considerable energy densities, more appropriate polarities than current biofuels such as ethanol, n-butanol, etc. and their volatility-ignition properties make these esters compatible for gasoline or diesel pools, depending on their alkyl group. In particular, pentyl valerate (PV) though has a lower energy density than fatty acid methyl esters (FAME), it shows a better volatility, cold-flow properties and lubricity benefits [7]. Besides, PV can be blended with diesel up to 20% without affecting the engine efficiency or emissions significantly [8].

The first work reporting PV production from GVL were based on hydrogenation to pentanoic acid (PA) and subsequent esterification of PA with pentanol (PL) using noble metal-based catalysts [7]. Then, an alternative route shown in Figure 1 was proposed by Chan-Thaw et al., comprising the reaction of GVL and PL in a one-pot process over Cu-based catalysts [9]. The first acid-catalyzed reaction of the Figure 1, starting from GVL, proceeds through the nucleophilic addition of the PL to the carboxylic group of GVL and ring-opening giving the intermediate 4-hydroxy pentyl valerate (HPV). The

second reaction, also promoted by acid sites, is the dehydration of HPV into pentyl 2-pentenoate (PP). This unsaturated ester can be hydrogenated to PV over metallic sites [9][10][11]. However, depending on the characteristics of the acid catalyst and reaction conditions, other byproducts can be formed such as 4-pentoxy pentyl valerate (PPV), 2-methyltetrahydrofurane (MTHF) and PA.

To the best of our knowledge, this reaction pathway towards PV has only been studied over Cu-based catalysts and using amorphous SiO_2-ZrO_2 [9], ZrO_2 [11] and $ZnAl_2O_4$ spinel [10] as supports. At the light of this, the one-pot conversion of GVL into PV in the presence of PL over Ni-based catalysts was studied in this work, focusing the research on the influence of the preparation method on the catalytic performance. Initially, a screening of different acid supports varying nature, density and strength of acid sites was carried out testing the GVL conversion to PP. Then, over the best acidic support, two Ni-based catalysts were prepared using: i) incipient wetness impregnation and ii) precipitation-deposition method to perform the one-pot production of PV from GVL and PL.

2. Materials and Methods

2.1. Materials and catalysts preparation

Commercial samples of SiO_2, γ-Al_2O_3 and SiO_2-Al_2O_3 were calcined in air flow (60 cm^3/min) at 773 K for 2 h before their use. ZnO(20%)/SiO_2 and HPA(42%)/SiO_2 samples were prepared by incipient wetness impregnation and then calcined.

Two different metal/acid bifunctional catalysts based on nickel and SiO_2-Al_2O_3 (SA) as support were prepared: Ni/SA-I by incipient wetness impregnation and Ni/SA-PD by the precipitation-deposition method. Precise information about all the materials, procedures and thermal treatments can be found in section SI.1 of Supporting Information.

2.2. Catalyst characterization

Elemental composition was determined by atomic absorption spectroscopy (AAS) and X-ray fluorescence spectroscopy (XRF). Textural properties were determined by sorptometry, the presence of crystalline phases in the solids was analyzed by X-ray diffraction (XRD), and particle size distribution of bifunctional catalysts was determined by dynamic image analysis. Regarding acid properties, surface acid density and relative strength of acid sites were determined by temperature programmed desorption (TPD) of NH_3 pre-adsorbed at 373 K and the Lewis/Brönsted acidity was analyzed by Fourier transform infrared spectroscopy (FT-IR) using pyridine as probe molecule. The relative reducibility of the calcined Ni-based samples was determined by temperature-programmed reduction (TPR). The H_2 chemisorption capacity of bifunctional samples was determined via volumetric adsorption experiments at room temperature. Transmission electron microscopy was also performed with the bifunctional samples. The details of the procedures and equipments involved in the experiments are provided in section SI.2 of Supporting Information and references within.

2.3. Catalytic tests

The conversion tests of GVL to PP and PV were performed in liquid phase and batch mode during 8 h at 523 K and 10 bar of H_2, using 1.5 mL GVL, 40 mL of pentanol (PL), 0.5 mL of hexadecane and 0.25 g of catalyst. Additional information such as reactor details, materials, reaction set-up, liquid sampling procedures, analysis of liquid samples and quantification of catalytic performance can be found in section SI.3 of Supporting Information and references within.

3. Results and discussion

The characterization results of acid solids are presented in section SI.4 and the results of the preliminary screening of these solids in the conversion of GVL into PP can be found in section SI.5 of Supporting Information. All these results led to the partial conclusion that the best acid solid to be used as support in the bifunctional catalytic system is SiO_2-Al_2O_3. This selection was based on its activity for converting GLV into HPV and then PP and its stability in the reaction medium. Then, now on SiO_2-Al_2O_3 employed as support is named SA.

3.1. Characterization results of the bifunctional Ni catalysts

The characterization results for the bifunctional Ni-based catalysts are presented in Table I. Ni content on Ni/SA-I and Ni/SA-PD, determined by AAS, was 7.3 and 8.2 wt%, respectively. Regarding textural properties, the specific surface area (S_g) decreased by 23.9% and 20.6% for Ni/SA-I and Ni/SA-PD, respectively, compared to the support value, whereas in the case of pore volume (V_P), a drop of 35.1% and 33.8%, respectively, was observed. This is indicating that the pores of the SiO_2-Al_2O_3 were partially blocked with Ni precursors during both preparation methods [12]. Regarding particle size, by dynamic image analysis it was determined that the average particle size was equal to 62, 64 and 67 μm for SA, Ni/SA-I and Ni/SA-PD, respectively, indicating that both preparation methods did not modify particle size significantly (Fig. SI.7). Besides, for both Ni/SA-I and Ni/SA-PD, as the SA support, the particles size showed to be smaller than 150 μm.

The X-Ray diffractograms of Ni/SA-I and Ni-SA/PD after calcination and reduction-passivation are shown in Figure 2. For the calcined Ni/SA-I sample, only the NiO polycrystalline phase was detected (PDF-2-44-1159) with a mean crystallite size of 10.4 nm, estimated by applying Scherrer's equation and considering the diffraction peak from NiO (0 1 2) planes (Table I). In contrast, for the calcined Ni/SA-PD sample

no diffraction peaks corresponding to NiO was observed, suggesting that NiO particles in Ni/SA-PD are smaller than 4 nm. Instead, diffraction signals assigned to a Ni hydrosilicate with a pecoraite structure ($Ni_3Si_2O_5(OH)_4$) usually called phyllosilicate was detected, in agreement with other authors [12][13]. For both reduced-passivated samples, a metallic Ni phase was detected (PDF-2-04-0850), with a mean Ni^0 crystallite size (from Ni (1 1 1) planes) of 8.1 and 5.0 nm for Ni/SA-I and Ni-SA-PD (Table I), respectively.

The TPR profiles of the calcined Ni/SA-I and Ni/SA-PD are presented in Figure 3. For Ni-SA-I two reduction peaks were observed. The first one, in the range 353-613 K and with the maximum H_2 consumption rate at 463 K related to particles of NiO having low interaction with the support [14], and the second one between 643 and 1083 K with the maximum at 783 K ascribed to the reduction of Ni^{2+} compounds strongly interacting with SiO_2-Al_2O_3 support [15]. Also for the Ni/SA-PD two reduction peaks were detected. However, the first one was between 353 K and 513 K (maximum at 437 K) related to Ni^{2+} species derived from the precipitation in the bulk of the solution during the preparation [25], and the second one between 653 K and 1053 K (with the maximum at 837 K) due to the reduction of the phyllosilicate phases [16]. At the light of the TPR results, the activation temperatures mentioned in section SI.1 were adopted for the bifunctional samples. It is worth mentioning that, generally, these phyllosilicate phases are not reduced completely after the activation process in the case of Ni/SA-PD samples, as other authors have previously reported [12]. In these cases, the authors observed the Ni^{2+} band by XPS determinations but, no diffraction lines were detected for the crystaline phase of phyllosilicates in XRD experiments, indicating that the particles of phyllosilicates are smaller than 4 nm.

The volume of hydrogen irreversibly chemisorbed on each reduced sample was equal to 2.7 and 4.0 $Ncm^3.g_{Ni}^{-1}$ for Ni-SA-I and Ni-SA-PD, respectively. It is clear that

the preparation method impacts strongly on the metallic dispersion. Assuming a stoichiometry H/Ni=1 [17] a Ni dispersion of about 5.0 and 12.3 % was estimated for the impregnated sample and the one prepared by precipitation-deposition, respectively.

Both activated/passivated Ni/SA catalysts were analyzed also by TEM and representative micrographs are presented in Figure SI.8 of Supporting Information. A wide distribution of Ni particle size was observed for Ni/SA-I sample (Fig. SI.8.a-c), containing from very small particles of about 9 nm to very large ones of approximately 70 nm. For Ni/SA-I catalyst the average Ni particle size was 24 nm (Table I and Fig. SI.8.g). In contrast, small Ni particles with a narrow distribution of sizes were observed for the Ni/SA-PD catalyst (Fig SI.8.d-f). In the case of this sample the Ni particle size was between 3 and 7 nm whereas the average size was about 5 nm (Fig. SI.8-h and Table I).

Finally, the relative strength and density of the acid sites present in the Ni-based reduced catalysts were studied by TPD of NH_3, and the results are shown in Figure 4 and Table I. The calcined SiO_2-Al_2O_3 exhibited a total acid site density of 0.59 μmol/m^2 (presented in Table SI.I) desorbing NH_3 in a wide range from 393 K up to 1073 K, with the maximum NH_3 desorption rate and a shoulder at 517 K and 697 K, respectively (Fig. 4). For the activated Ni/SA-I the distribution of the strength of the sites became narrower respect to the bare support, desorbing NH_3 between 393 K and about 863 K (Fig. 4). Although the position of the maximum desorption rate did not change (T=517 K), the total acid site density for Ni/SA-I was maintained due to the increase in the intensity of the desorption band, showing a total acid site density (n_A=0.60 μmol/m^2) very similar to that of the support. In contrast, for the Ni/SA-PD both the temperature of the maximum desorption rate and the intensity of the desorption band diminished (Fig. 4). The temperature of the maximum desorption rate was 483 K, .i.e. 34 K lower than in Ni/SA-I and the total acid site density was 0.31 μmol/m^2, half of the value

corresponding to Ni/SA-I. In summary, for a similar Ni loading on the SiO_2-Al_2O_3, the higher the Ni dispersion, the lower total acid site density. Even more, when the Ni dispersion is higher, i.e. in the case of Ni/SA-PD, the relative acid strength diminishes considerably.

It is worth mentioning that a significant modification of the L/(L+B) ratio in the bifunctional Ni catalysts in comparison with the value of the support is not expected in this case. Other authors have reported modifications in the Lewis/Brönsted balance or the L/(L+B) ratio, when the Ni catalysts are prepared by ion exchange [18] or by coimpregnation of Ni and promoters such as Cr, Mo or W [19]. For the particular case of impregnated Ni-based catalysts, Castaño et al reported for a Ni(24%)/SA-I a L/(L+B) ratio equal to 0.95, whereas the value for the bare SA support was 0.85 [20]. However, in our case, the Ni loading was about 8% so it is expected that this difference would be even smaller. In addition, the difference in the degree of reduction of the Ni oxide species (such as NiO or $Ni_3Si_2O_5(OH)_4$) between Ni/SA-I and Ni/SA-PD can be as much as 15% [12][21]. In this sense a slightly higher L/(L+B) ratio could be expected for Ni/SA-PD due to a higher surface concentration of Ni^{2+} oxide especies. Nevertheless, these especies are located over SiO_2-Al_2O_3 with L/(L+B)=0.79. Thus, new Lewis acid sites by the presence of unreduced $Ni_3Si_2O_5(OH)_4$ could be created but they would be covering the acid sites of the support (mainly Lewis), modifying the overall L/(L+B) balance of the bifunctional catalyst only slightly. This fact, in a completely different way, was experimentally verified by the product distribution that Bertone et al have detected during certain reactions over this kind of samples [12][21].

3.2. Catalytic results for the conversion of GVL to PV over bifunctional catalysts

The one-pot conversion of GVL into PV in the presence of pentanol and H_2 was performed over the bifunctional Ni-based catalysts and the results are presented in

Figure 5. Both catalysts were active in these experimental conditions. However, Ni/SA-I was appreciable more active than Ni/SA-PD. For the latter, the initial GVL conversion rate, estimated by polynomial fitting of the curves concentration vs. time and differentiation at zero time, was r^0_{GVL}= 3.66 x10^{-3} mol/g.h, whereas the initial PV formation rate was r^0_{PV}= 3.07 x10^{-3} mol/g.h. Taking into account the values of the acid site density (n_A) and metal dispersion (D_M) presented in Table I, initial TOF values for GVL conversion and PV formation were equal to 32.3 h^{-1} and 17.9 h^{-1}, respectively. The GVL conversion after 8 h over Ni/SA-PD was 40.9% with a PV yield of 29.3%, showing a PV selectivity of about 71.6%. The carbon balance after 8 h of reaction was estimated in 99.9% (Fig. 5).

In the case of Ni/SA-I, the initial GVL conversion rate was equal to r^0_{GVL}= 2.39 x10^{-2} mol/g.h whereas the initial PV formation rate was r^0_{PV}= 4.39 x10^{-3} mol/g.h. In other words, Ni/SA-I, with an acid site density twice that of Ni/SA-PD sample, converted GVL 6.5 times faster than the latter but the formation of PV was only 1.4 times faster. Considering the values of the acid site density (n_A) and metal dispersion (D_M) of Table I, in the case of Ni/SA-I initial TOF values for GVL conversion and PV formation were equal to 113.3 h^{-1} and 70.6 h^{-1}, respectively. It is worth mentioning that the initial TOF for GVL conversion over Ni/SA-I was very similar than that of the SA support (118.7 h^{-1}), with a very similar total acid site density. This fact could be use as a confirmation that the L/(L+B) ratio of Ni/SA-I is not very different from that of the SA support [22], at the light of the total acid site density n_A is practically the same. After 8 h of reaction, Ni/SA-I converted the 67.0% of the GVL, reaching a PV yield of 55.1%. With these values, the PV selectivity was 82.2% with a carbon balance after 8 h of 99.5% (Fig. 5). In summary, the GVL conversion rate over the bifunctional catalyst was strongly affected by the acid site density that, for a similar Ni content, depends markedly on the Ni dispersion and, consequently, on the preparation method.

It is relevant to mention that during a blank hydrogenation test, converting GVL over SA support in the presence of H_2, no PV formation was observed, showing that metallic parts of the reactor do not catalyze the hydrogenation. This test confirmed the hydrogenation activity of Ni^0 phase in Ni/SA-I and Ni/SA-PD for converting the intermediate PP into the valuable PV. At the light of the low PP yield (lower than 1-2%) observed in all the experiments converting GVL into PV in the presence of pentanol and H_2, it is likely that PP obtained over acid sites reacts very fast with chemisorbed H on neighbouring Ni^0 particles.

Based on the fact that both Ni/SA catalysts were significantly selective to PV (S_{PV}>71%) but Ni/SA-I was more active and relatively more selective (S_{PV}>82.2%), a 24 h-catalytic run was carried out using this sample, and the results are shown in Figure SI.6. In this case, a final GVL conversion of 83.5 % was reached, with a PV yield of 73.3% and selectivity to PV of 87.8%. The maximum yield of the undesirable product PPV was 8.8%. Besides, small amounts of AP were only observed at the beginning of the experiment in concentration similar to the HPV intermediate (<3%). The carbon balance at the end of this run was 99.8%, indicating that the amount of reactant, intermediates, products or by-products coming from GVL that remained strongly adsorbed was very low. Chan-Thaw et al. reported 72% PV selectivity as the highest value in their study with a GVL conversion of 92% after 20 h of reaction [9]. These authors explained their results by the presence of Lewis acid sites after deposition of the CuO phase on the silica modified with ZrO_2. In this work, it was observed that the impregnation of SiO_2-Al_2O_3 with Ni solution during preparation of Ni/SA-I did not modify strongly the total acid site density (Table I), though the range for the NH_3 desorption band became narrower respect to the bare support (Fig. 4). Even more, another difference with the findings of Chan-Thaw et al. was observed in the acid requirements for the acid-catalyzed reactions. In our case it was verified that both

Lewis and Brønsted acid sites are necessary to produce the PP intermediate whereas in the Cu-SiZr catalysts the active acid sites were exclusively Lewis sites [9]. In this sense, our findings regarding acid sites requirements are similar to the ones of Li et al. using Cu supported on ZrO_2-$ZnAl_2O_4$ composites, who reported a surface cooperation catalytic mechanism between Lewis/Brönsted acid sites and highly dispersed copper species that boosted the GVL conversion up to 91% with a PV selectivity of 99% after only 10 h [10].

Finally, in order to verify whether some deactivation process takes place in Ni/SA-I sample a re-use test, using 0.5 g of catalyst, was performed where the catalyst was used three consecutive times during 7 h, and the results are presented in Figure 6. The GVL conversion diminished from 75.2% in the first reaction cycle to 59.2% in the third cycle. The drops for PV yield and PV selectivity from the first cycle to the third were about to 30.2% and 28.6%, respectively. At the time being further studies focussing the attention on the deactivation of this sample are being carried out in order to have a deeper knowledge of this phenomenon. It is important to mention that no significant leaching of Ni was detected performing AAS analysis of the reaction mixture when Ni/SA-I and Ni/SA-HD were used as catalysts. In all the cases, the Ni concentration in the reaction mixture at the end of runs was lower than the detection limit of the technique (0.01 mg/L).

These are promising results for continuing exploring the one-pot PV production from GVL and PL over Ni-based catalysts. From a comparison of the results obtained in this work and the findings of other authors it is clear that for achieving a higher activity and selectivity to PV from GVL and PL over Ni/SA it is necessary to precisely tune up the density of acid sites (Lewis and Brønsted) on the support by adjusting the Ni dispersion, in order to optimize the interaction between the surface intermediates and chemisorbed hydrogen. This challenging task will be matter of a future study.

4. Conclusions

The one-pot conversion of γ-valerolactone to pentyl valerate biofuel in the presence of pentanol is efficiently promoted by Ni-based bifunctional catalysts at 523 K and 10 bar of partial hydrogen pressure. SiO_2-Al_2O_3 (SA) support, with an appreciable activity, selectivity and stability in the reaction medium is an appropriate support for promoting the two-step consecutive conversion of γ-valerolactone into pentyl 2-pentenoate over the acid sites, whereas Ni^0 sites are active for the hydrogenation of pentyl 2-pentenoate into pentyl valerate.

The preparation method of Ni-bifunctional catalysts impacts dramatically on the catalytic activity in the one-pot production of pentyl valerate from γ-valerolactone and pentanol. Precipitation-deposition (PD) method, leading to a higher Ni dispersion, reduces significantly the acid site density in bifunctional Ni/SA-PD catalyst and consequently the catalytic performance. In contrast, by incipient wetness impregnation a poorly dispersed Ni/SA-I catalyst is obtained with a significantly better performance. However, the preparation method does not impact so strongly on the catalytic selectivity, reaching a pentyl valerate selectivity of 71.6% and 82.2% for Ni/SA-PD and Ni/SA-I, respectively. Finally, during a 24 h run over Ni/SA-I a γ-valerolactone conversion of 83.5% with a pentyl valerate selectivity of 87.8% can be achieved. These promising results confirm that in order to allow an efficient interaction between surface intermediates, acid sites and chemisorbed hydrogen on Ni^0, the Ni dispersion must be precisely tuned up for achieving high activity and selectivity and reducing the deactivation observed during three reaction cycles.

Acknowledgements

The authors thank Universidad Nacional del Litoral (Grant CAI+D 2016-PI 50420150100061LI), Consejo Nacional de Investigaciones Científicas y Técnicas (Grant PIP 2015-11220150100767CO), and Agencia Nacional de Promoción Científica y Tecnológica (Grant PICT-2015-3545 from ANPCyT) from Argentina, for the financial support.

Thanks are also given to LMA-INA-UNIZAR and Victor Sebastian for the transmission electronic microscopy analyses.

References

[1] S. Zinoviev, F. Müller-Langer, P. Das, N. Bertero, P. Fornasiero, M. Kaltschmitt, G. Centi, S. Miertus, ChemSusChem. 3 (2010) 1106–1133.

[2] T.N. Pham, D. Shi, D.E. Resasco, Appl. Catal. B Environ. 145 (2014) 10–23.

[3] K. Yan, Y. Yang, J. Chai, Y. Lu, Appl. Catal. B Environ. 179 (2015) 292–304.

[4] A. Rozenblit, A.J. Avoian, Q. Tan, T. Sooknoi, D.E. Resasco, J. Energy Chem. 25 (2016) 1008–1014.

[5] J.Q. Bond, D. Martin Alonso, R.M. West, J.A. Dumesic, Langmuir 26 (2010) 16291–16298.

[6] J.Q. Bond, D. Wang, D.M. Alonso, J.A. Dumesic, J. Catal. 281 (2011) 290–299.

[7] J.P. Lange, R. Price, P.M. Ayoub, J. Louis, L. Petrus, L. Clarke, H. Gosselink, Angew. Chemie - Int. Ed. 49 (2010) 4479–4483.

[8] F. Contino, P. Dagaut, G. Dayma, F. Halter, F. Foucher, C. Mounaïm-Rousselle, J. Energy Eng. 140 (2014) 1–7.

[9] C.E. Chan-Thaw, M. Marelli, R. Psaro, N. Ravasio, F. Zaccheria, RSC Adv. 3 (2013) 1302–1306.

[10] W. Li, Y. Li, G. Fan, L. Yang, F. Li, ACS Sustain. Chem. Eng. 5 (2017) 2282–2291.

[11] S. Liu, G. Fan, L. Yang, F. Li, Appl. Catal. A Gen. 543 (2017) 180–188.

[12] M.E. Bertone, C.I. Meyer, S.A. Regenhardt, V. Sebastian, T.F. Garetto, A.J. Marchi, Appl. Catal. A Gen. 503 (2015) 135–146.

[13] A.J. Majewski, J. Wood, W. Bujalski, Int. J. Hydrogen Energy 38 (2013) 14531–14541.

[14] R. Fréty, L. Tournayan, M. Primet, G. Bergeret, M. Guenin, J.B. Baumgartner, A. Borgna, J. Chem. Soc. Faraday Trans. 89 (1993) 3313–3318.

[15] S.A. Regenhardt, C.I. Meyer, T.F. Garetto, A.J. Marchi, Appl. Catal. A Gen. 449 (2012) 81–87.

[16] A. Gil, A. Díaz, L.M. Gandía, M. Montes, Appl. Catal. A, Gen. 109 (1994) 167–179.

[17] C.I. Meyer, S.A. Regenhardt, A.J. Marchi, T.F. Garetto, Appl. Catal. A Gen. 417–418 (2012) 59–65.

[18] A. Martínez, M.A. Arribas, P. Concepción, S. Moussa, Appl. Catal. A Gen. 467 (2013) 509–518.

[19] V.K. Velisoju, D. Jampaiah, N. Gutta, U. Bentrup, A. Brückner, S.K. Bhargava, V. Akula, ChemCatChem 12 (2020) 1341–1349.

[20] P. Castaño, B. Pawelec, J.L.G. Fierro, J.M. Arandes, J. Bilbao, 86 (2007) 2262–2274.

[21] M.E. Bertone, S.A. Regenhardt, C.I. Meyer, V. Sebastian, T.F. Garetto, A.J. Marchi, Top. Catal. 59 (2016) 159–167.

[22] D.J. Segobia, A.F. Trasarti, C.R. Apesteguía, Chinese J. Catal. 40 (2019) 1693–1703.

Table I: characterization results for the bifunctional Ni-based catalysts.

Sample	Ni load[(a)] (wt%)	S_g[(b)] (m^2/g)	V_P[(c)] (cm^3/g)	L_{NiO}[(d)] (nm)	L_M^0[(e)] (nm)	T_{MAX}[(f)] TPR (K)	D_M[(g)] (%)	n_a TPD[(h)] ($\mu mol/m^2$)	d_{Ni0}[(i)] (nm)
Ni/SA-I	7.3	350	0.48	10.4	8.1	463 / 783	5.0	0.60	24
Ni/SA-PD	8.2	365	0.49	-	5.0	437 / 837	12.3	0.31	5

[(a)] Ni loading determined by AAS. [(b)] Specific surface area determined by BET method. [(c)] Pore volume determined by BJH method. [(d)] Crystallite size of metal oxide estimated by applying the Scherrer's equation. [(e)] Estimated Ni^0 particle size by applying the Scherrer's equation. [(f)] Maximum temperatures in TPR profiles. [(g)] Metal dispersion estimated by H_2 chemisorption assuming a 1:1 Ni:H stoichiometry. [(h)] Acid sites density estimated by NH_3 TPD. (i) Metallic Ni average particle size estimated from TEM images by counting 100-130 particles.

Figures Captions

Fig. 1: Reaction network for the one-pot production of pentyl valerate (PV) from biomass-derived γ-valerolactone (GVL) over bifunctional metal/acid catalysts [➡ metal catalyst; ➡ acid catalyst].

Fig. 2: X-ray diffraction (XRD) patterns of calcined and activated/pasivated Ni-based samples [(●) NiO (PDF-2-44-1159); (**O**) $Ni_3Si_2O_5(OH)_4$ (PDF-2-22-0754); (■) Ni^0 (PDF-2-04-0850); scan speed: 2°/min].

Fig. 3: Temperature-programmed reduction (TPR) of calcined Ni-based samples [heating rate: 10 K/min; flow rate: 60 cm^3/min of H_2(5%)/Ar].

Fig. 4: Temperature-programmed desorption (TPD) of NH_3 from bare support and Ni-based catalysts [heating rate: 10 K/min, flow rate: 30 cm^3/min (He)].

Fig. 5: Catalytic activity results for the conversion of GVL into PV over Ni/SA-I and Ni/SA-PD catalysts [T=523 K, p=10 bar (H_2), W_C=0.25 g, V_{PL}=40 mL, C^0_{GVL}= 0.37 M, stirring rate= 650 rpm, time= 8 h].

Fig. 6: Re-use tests for Ni/SA-I catalyst in the conversion of GVL into PV during three reaction cycles [T=523 K, p=10 bar (H_2), W_C=0.50 g, V_{PL}=40 mL, C^0_{GVL}= 0.37 M, stirring rate= 650 rpm, time= 7 h].

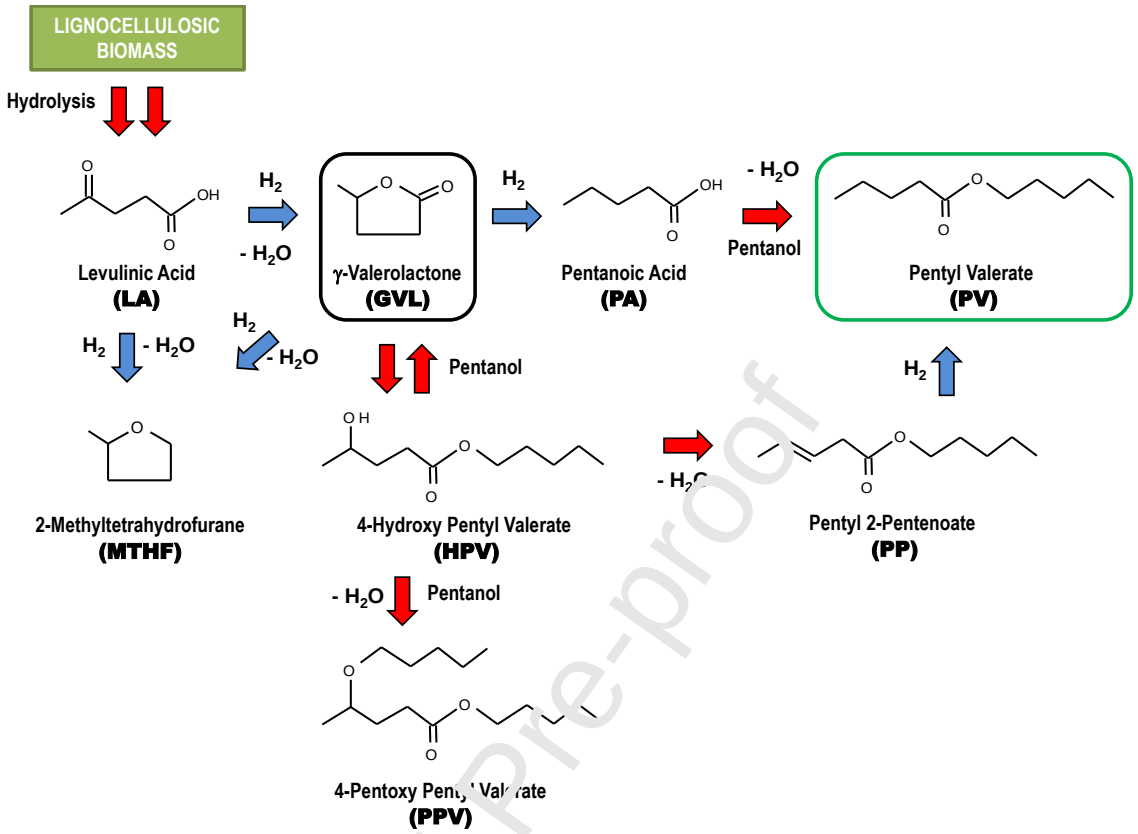

Figure 1

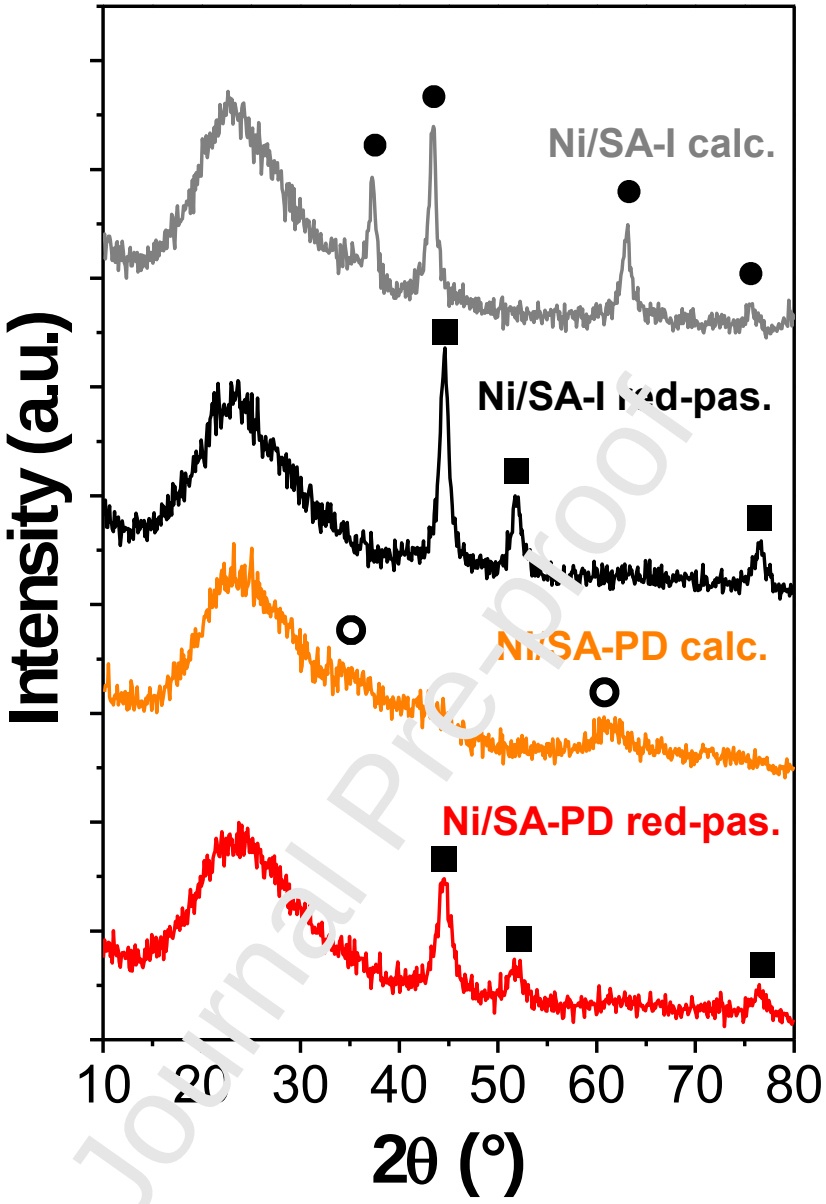

Figure 2

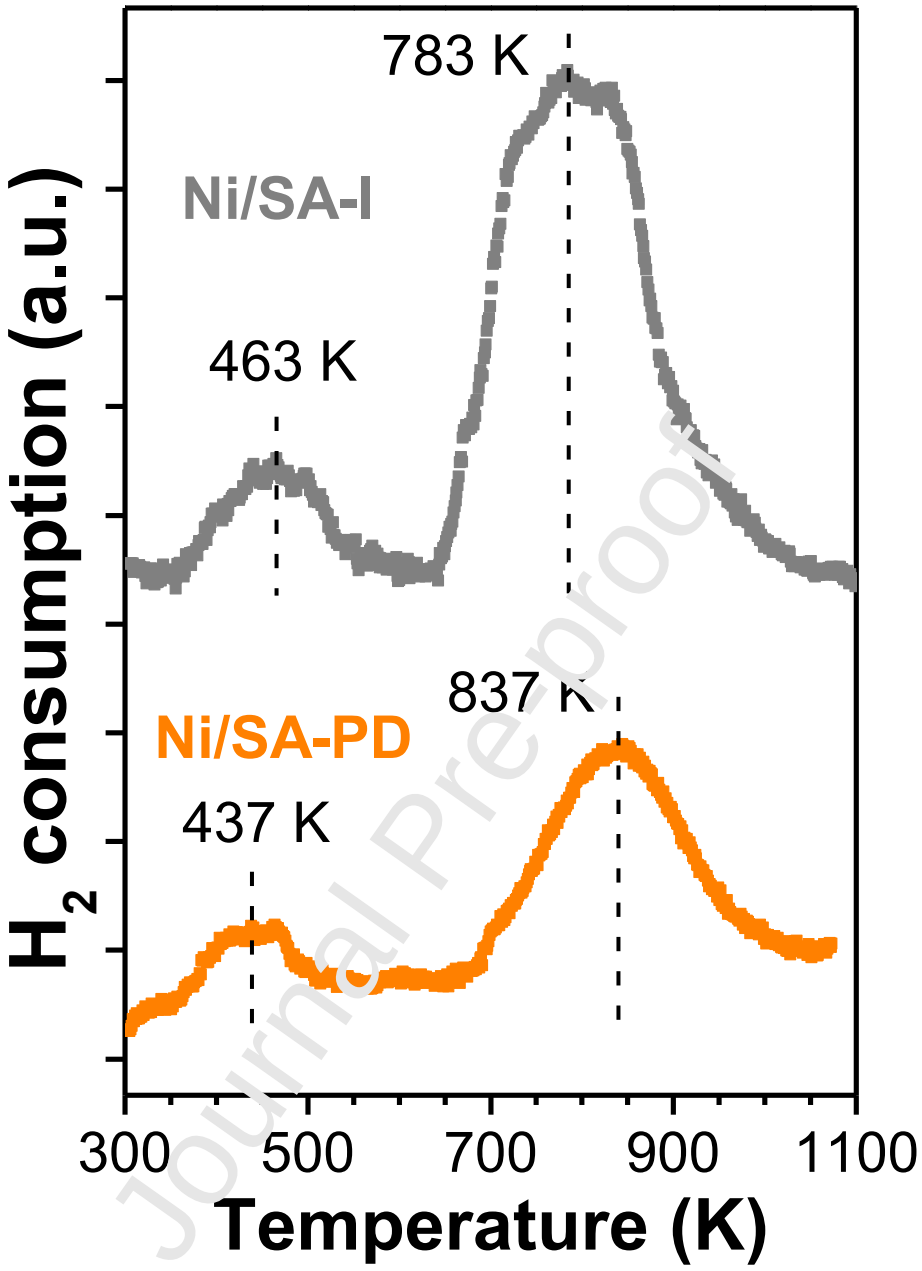
783 K
Ni/SA-I
463 K
837 K
Ni/SA-PD
437 K
H2 consumption (a.u.)
300
500
700
900
1100
Temperature (K)

Figure 3

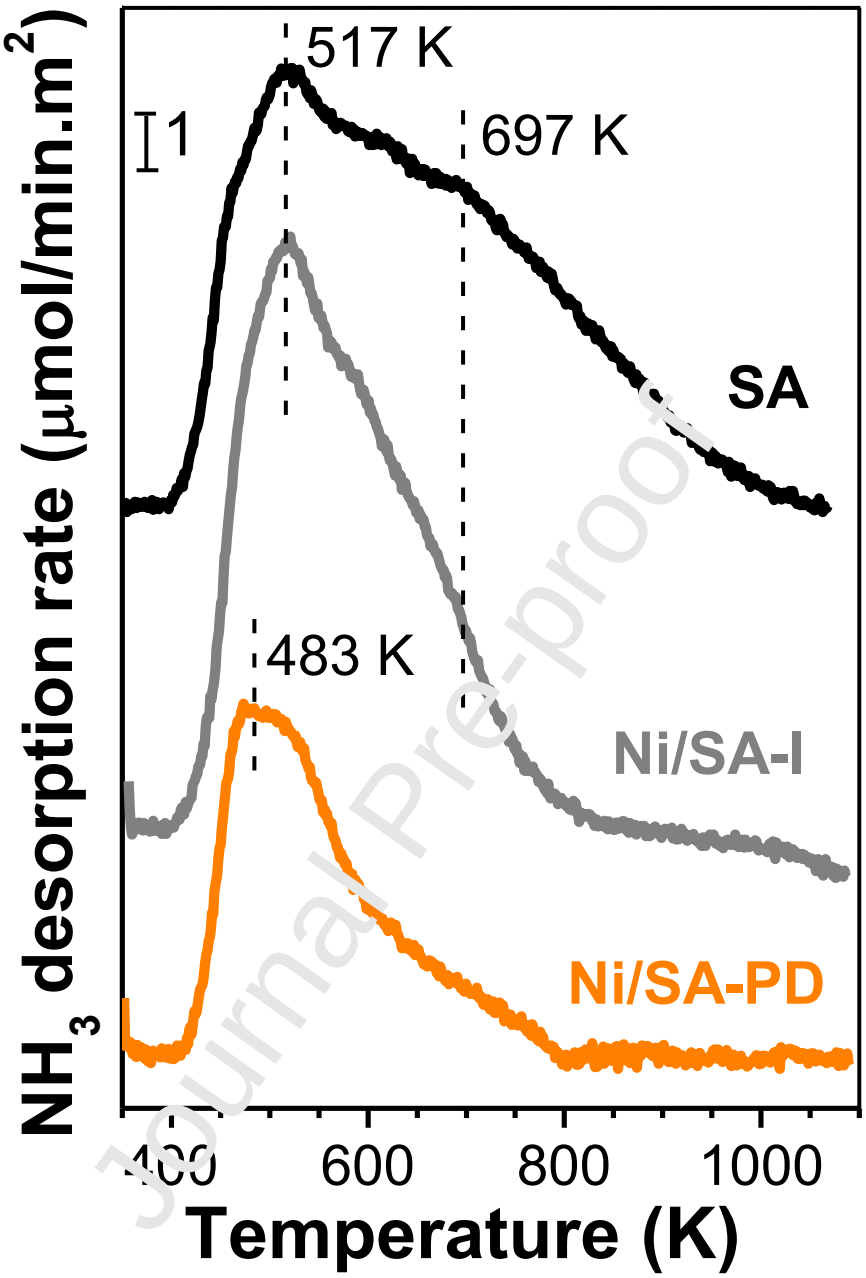
517 K
1
697 K
SA
483 K
Ni/SA-I
Ni/SA-PD
600
800
1000
Temperature (K)
NH3 desorption rate (μmol/min.m2)

Figure 4

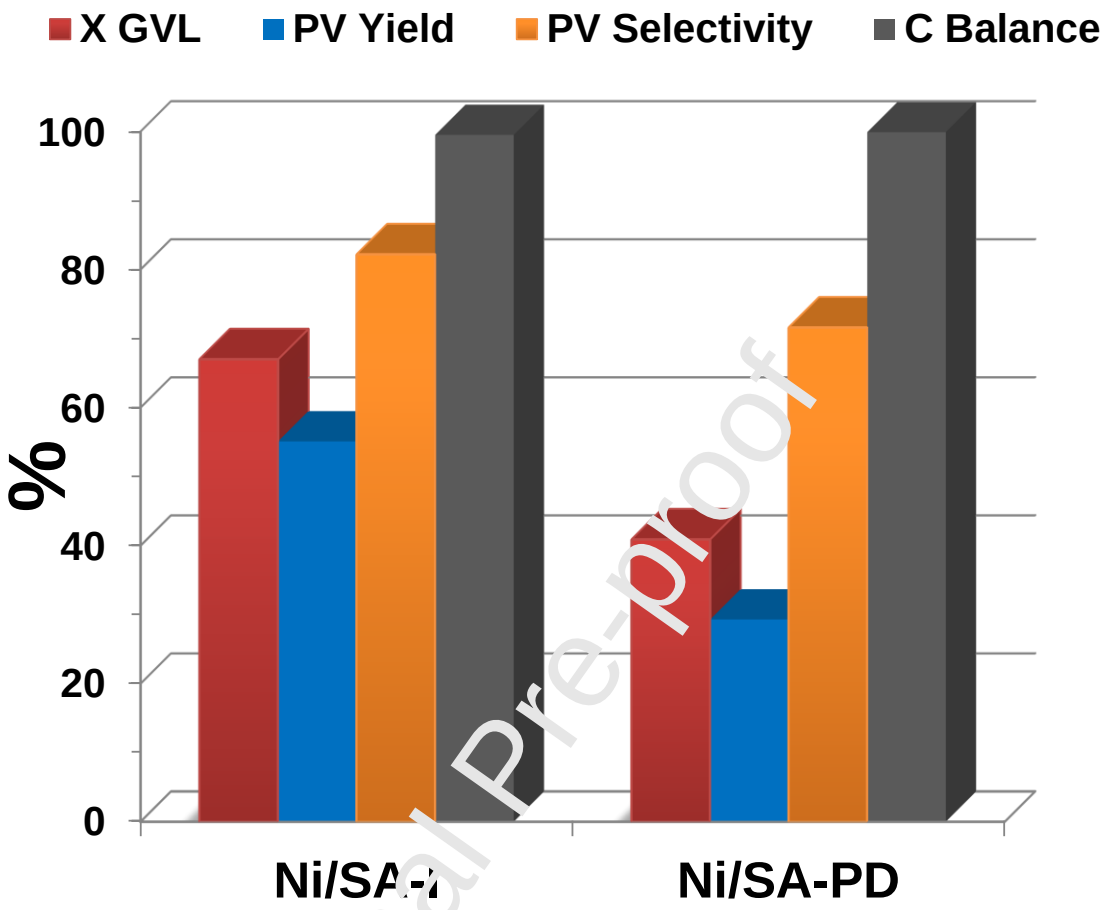

Figure 5

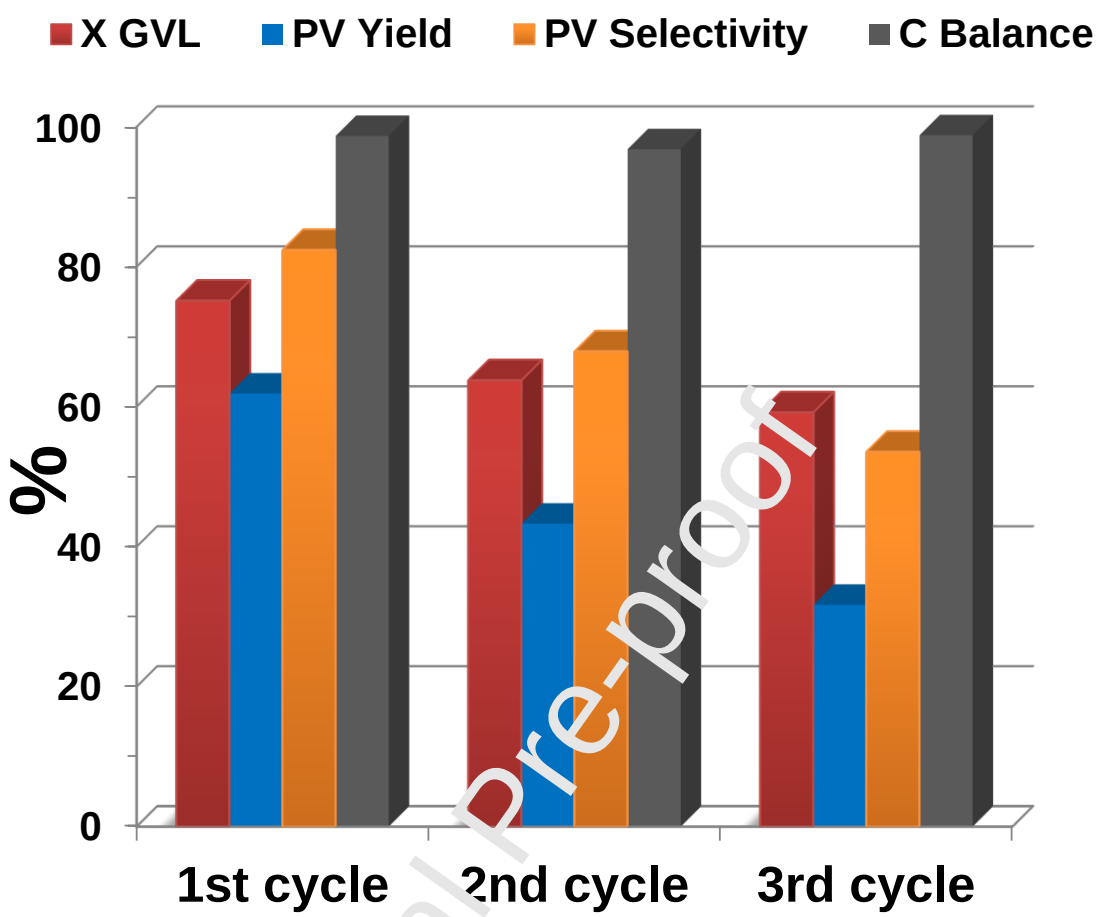

Figure 6

Research Highlights

- Nucleophilic addition of pentanol to γ-valerolactone requires Lewis and Brønsted acidity
- Pentyl-2-pentenoate is hydrogenated fast to pentyl valerate over Ni/SiO_2-Al_2O_3
- Preparation method of Ni/SiO_2-Al_2O_3 impacts strongly on the density of acid sites
- Impregnated Ni/SiO_2-Al_2O_3 is more active than prepared by precipitation-deposition
- Impregnated Ni/SiO_2-Al_2O_3 achieved 87.8% selectivity to pentyl valerate after 24 h

CRediT author statement

Karla Geraldyne Martínez Figueredo: Validation, Formal analysis, Investigation, Writing - Review & Editing, Visualization
Darío Jobino Segobia: Methodology, Validation, Writing - Review & Editing
Nicolás Maximiliano Bertero: Conceptualization, Methodology, Resources, Writing - Original Draft, Visualization, Supervision, Project administration, Funding acquisition

Declaration of interests

☒ Karla G. Martínez Figueredo, Darío J. Segobia and Nicolás M. Bertero declare that they have no known competing financial interests or personal relationships that could have appeared to influence the work reported in this paper.

☐The authors declare the following financial interests/personal relationships which may be considered as potential competing interests:

Graphical Abstract